Available online at www.sciencedirect.com
ScienceDirect
Cement and Concrete Research 37 (2007) 38–46
Cement and Concrete Research

Characterization of multi-scale porosity in cement paste by advanced ultrasonic techniques

Wonsiri Punurai [a,b], Jacek Jarzynski [c], Jianmin Qu [c], Jin-Yeon Kim [c], Laurence J. Jacobs [a,c], Kimberly E. Kurtis [a,*]

[a] School of Civil and Environmental Engineering, Georgia Institute of Technology, Atlanta, GA 30332, United States
[b] Department of Civil Engineering, Mahidol University, Nakornpathom, Thailand
[c] G.W. Woodruff School of Mechanical Engineering, Georgia Institute of Technology, Atlanta, GA 30332, United States

Received 17 April 2006; accepted 20 September 2006

Abstract

The effectiveness of advanced ultrasonic techniques to quantitatively characterize the capillary porosity and entrained air content in hardened cement paste is examined. Direct measurements of ultrasonic attenuation are used to measure the volume fraction and average size of entrained air voids and to assess variations in intrinsic porosity – as influenced by water-to-cement ratio (w/c) – in hardened cement paste samples. For the air entrained specimens, an inversion procedure based on a theoretical attenuation model is used to predict the average size and volume fraction of entrained air voids in each specimen, producing results in very good agreement with results obtained by standard petrographic methods and by gravimetric analysis. In addition, ultrasonic attenuation measurements are related to w/c to quantify the relationship between increasing porosity (with increasing w/c) and ultrasonic wave characteristics.

Keywords: Admixture (D); Air entrainment; Microstructure (B); Pore size distribution (B); Modelling (E)

1. Introduction

Accurate field measurements of entrained air characteristics and water-to-cement ratio (w/c) in concrete mixtures are important to ensure that specifications for workability, strength, and durability are met [1]. However current standard methods for characterizing concrete in the field may not provide adequate information regarding the composition and structure of in-place concrete. For example, the w/c of a fresh concrete mixture is typically assessed indirectly in the field by the slump test, which is sensitive to the water content but is also sensitive to the cement content, aggregate gradation, environmental conditions, the use of chemical admixtures and/or supplementary cementitious materials (SCMs), among other factors. Also, field measurements to characterize the w/c and air content of concrete are commonly performed prior to placement, compaction, and finishing and may not always accurately reflect the actual properties of the in-place material. Finally, with regard to characterization of air entrainment, most standard field methods for measuring air content, including ASTM C138 gravimetric method [2], ASTM C173 volumetric or rollometer method [3], and ASTM C231 pressure method [4], cannot differentiate between entrained and entrapped air, and this distinction can be critical for evaluating the durability of concrete to freeze/thaw cycles. Of course, petrography [5] can be used to measure both entrained air content and w/c in hardened concrete, but an on site test could provide results more rapidly and at potentially lower cost.

Advanced ultrasonic methods have the potential to be fast, reliable and inherently safe tools for providing quantitative information about the initial characteristics of plastic and in-place fresh concrete microstructure and, subsequently, for in situ condition assessment. A number of researchers [6–14] have recently developed correlations between ultrasonic wave properties, such as phase velocity and attenuation, with characteristics

* Corresponding author. Tel.: +1 404 385 0825.
E-mail address: kimberly.kurtis@ce.gatech.edu (K.E. Kurtis).

0008-8846/$ - see front matter © 2006 Elsevier Ltd. All rights reserved.
doi:10.1016/j.cemconres.2006.09.016

Table 1
Specimen specifications

Name	w/c	Air-entraining agent (% by cement mass)	Diameter (mm)	Thickness (mm)
CP1	0.3	–	100	23.1–25.5
CP2	0.4	–	100	23.3–24.7
CP3	0.5	–	100	23.2–26.5
CP4	0.6	–	100	22.5–24.8
EACP1	0.4	0.2	100	23.6–26.5
EACP2	0.4	0.6	100	24.7–26.2
EACP3	0.4	1	100	22.7–24.8

such as stiffness, porosity and w/c. However, the development of quantitative measurement techniques based upon these ultrasonic wave properties has not generally been addressed for cement-based materials. An important aim of this research, then, is to enable the quantitative and direct measurement of entrained air void size and volume fraction in hardened cement paste through the development of an inversion procedure which couples an established ultrasonics scattering model with experimentally measured attenuation values.

In this research, ultrasonic attenuation is used to characterize the average size and volume fraction of entrained air voids in cement paste of a single w/c, and then to characterize how variations in w/c (and concomitant variations in intrinsic porosity) influence attenuation. There are two basic mechanisms by which an ultrasonic wave attenuates: geometric attenuation and material attenuation. Geometric attenuation is the phenomenon by which the amplitude of an ultrasonic wave decreases as the wavefront spreads out over a wider area. Material attenuation can be classified as either absorption or scattering. One source of absorption losses is internal friction in a viscoelastic material, while scattering losses are highly complex, and are dependent upon the intrinsic length scale of the scatterer, the volume and distribution of scatterers, and the acoustic properties of these scatterers in relationship to the matrix material. Since these two effects (absorption and scattering) are coupled, any attenuation measurements will inevitably include both contributions.

The objectives of this research are to examine the effectiveness of advanced ultrasonic techniques to measure the average size and volume fraction of entrained air voids in cement paste and to examine how ultrasonic measurements are affected by intrinsic porosity, as influenced by variations in w/c. Direct ultrasonic attenuation measurements are performed on a set of hardened cement paste specimens at constant w/c with entrained air void contents that vary between 0 and 15%. An inversion procedure – based on a theoretical attenuation model and following the measurement procedure developed in [15,16] is used to predict the average size and volume fraction of entrained air voids in each specimen. The accuracy of these ultrasonic predictions is verified with a direct comparison to results obtained by petrographic analysis on the hardened pastes (ASTM C457-98, method B [5]) and by gravimetric analysis of the fresh pastes. In addition, attenuation measurements made on cement pastes prepared at w/c ranging from 0.30 to 0.60 aid in quantifying the relationship between cement paste microstructure and ultrasonic wave characteristics.

2. Experimental description

2.1. Specimen characteristics

Paste specimens were produced according to mixture proportions listed in Table 1. A practical range of entrained air void contents (by volume, ϕ) and w/c were selected. All mixtures were prepared using commercially available Type I portland cement and water. The specimens denoted in Table 1 with an "EACP" prefix include varying dosages of a chemical air-entraining admixture. The specimens denoted in Table 1 with a "CP" prefix do not contain the air-entraining agent, but were prepared at 4 different w/c.

All mix ingredients were weighed to 0.1 mg accuracy, and mixing was performed using a Hobart paddle mixer. Samples were cast in 100 mm × 200 mm plastic cylinder molds, which were covered with plastic caps and kept in a moist environment for 24 h at 22 °C and 76% RH. At 24 h of age, all specimens were demolded and were subsequently stored in an environmentally-controlled fog room for 27 more days at 22 °C. At 28 days of age, all specimens were removed and a water-cooled diamond saw was used to cut 22.5–

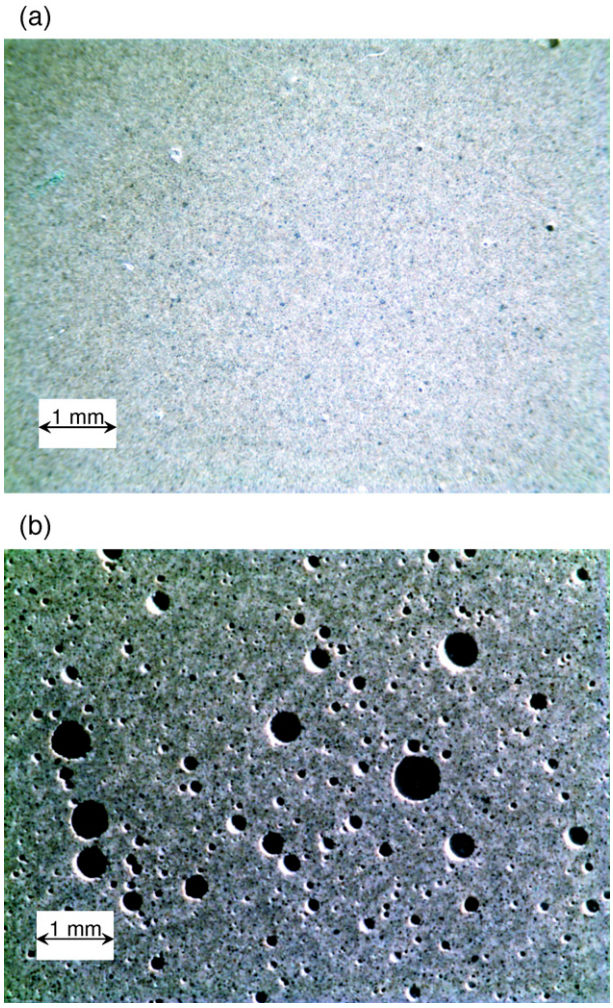

Fig. 1. Magnified digital images of two specimens (a) CP2 and (b) EACP2.

26.5 mm thick samples from the cast cylinders. The saw cut surfaces of the specimens were polished using progressively finer silicon carbide grit (ending with #600) producing two parallel surfaces to allow through transmission of ultrasonic waves without reflections from the sample sides. Note that between ultrasonic tests, the specimens were stored in a sealed container at 75±2% RH.

Fig. 1 shows magnified images of two specimen surfaces – a plain cement paste sample (CP2) and an air entrained cement paste sample (EACP2). These representative images demonstrate the relatively more homogeneous cement paste matrix characteristic of the CP samples, as well as the size and spacing of the entrained air voids in the EACP specimens.

2.2. Ultrasonic measurement procedure

A schematic diagram of the experimental setup for the attenuation measurements is shown in Fig. 2. In brief (see Ref. [15] for details), a pair of commercially available contact ultrasonic transducers (labeled T for transmitting and R for receiving) were located on axis (epicenter) on opposite faces of each specimen. Two matched pairs of broadband transducers (one pair with a nominal center frequency of 2 MHz, and a second pair with a nominal center frequency of 5 MHz) were used to generate and detect longitudinal ultrasonic waves. A typical time-domain signal is shown in Fig. 2 where the contributions from the direct propagation (with a propagation distance of one thickness, z) and the twice reflected component

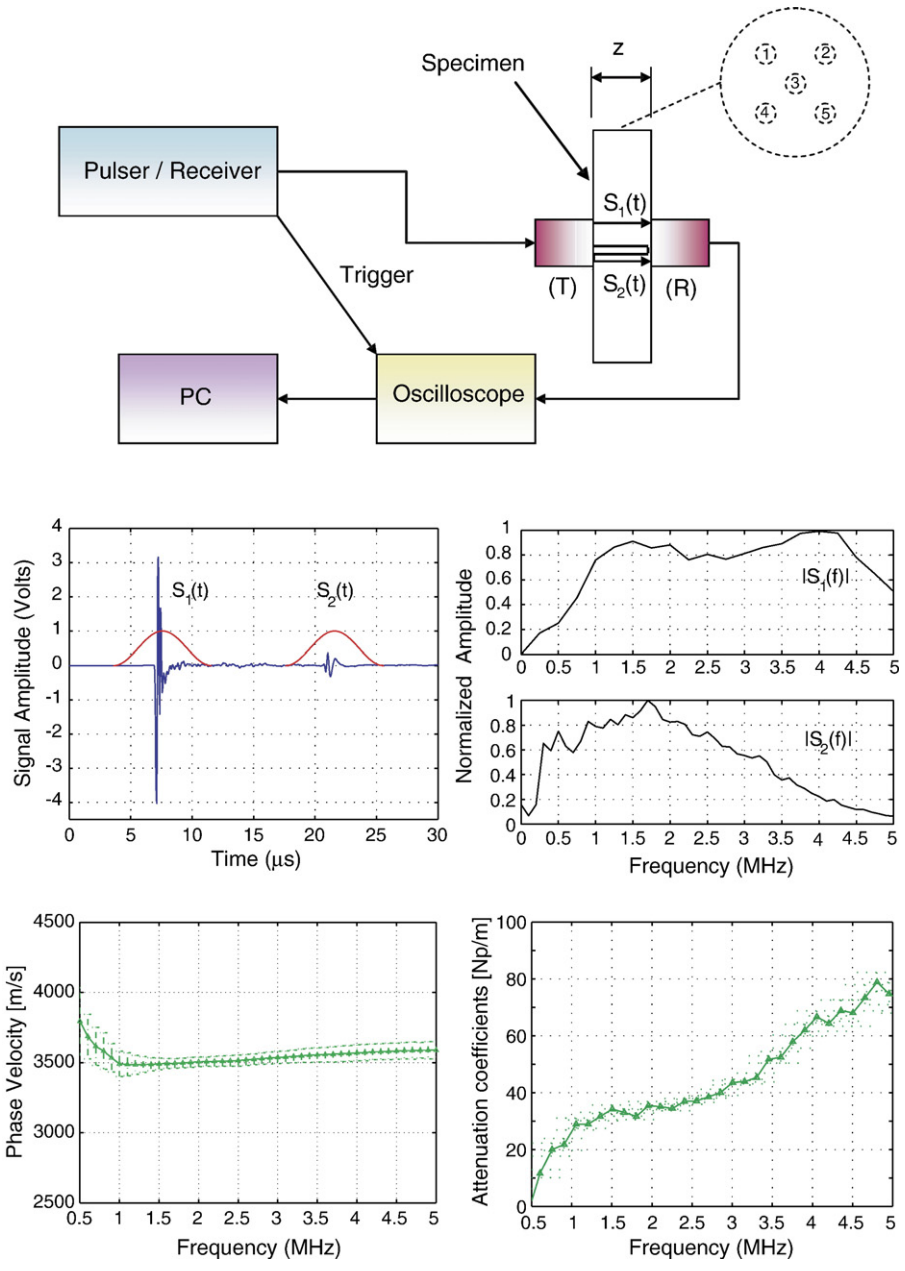

Fig. 2. A schematic diagram of the experimental setup for the attenuation measurements.

(that propagates three-thicknesses, $3z$) are identified as $S_1(t)$ and $S_2(t)$, respectively. The attenuation analysis (detailed in [15]) compares the frequency-dependent amplitudes of these two contributions (which are Hanning windowed and diffraction corrected) to obtain the experimentally measured phase velocity and attenuation. Typical plots of these intermediate steps are shown in Fig. 2, and note that the measured attenuation (in Nepers/m) is the total attenuation, containing both the absorption and scattering contributions.

2.3. Theoretical attenuation model and inversion procedure

The theoretical relationship between ultrasonic attenuation and the size and volume fraction of entrained air voids is based on the model proposed in Ref. [17]. Following Ref. [15], the total attenuation, α, of a longitudinal ultrasonic wave in these specimens is a combination of the absorption contribution α_a, occurring in the cement paste matrix, and the scattering contribution α_s, due to the presence of a volume fraction, ϕ of entrained air voids. This relationship can be described by

$$\alpha = \alpha_a + \alpha_s = (1-\phi)\alpha_a + \frac{1}{2} n_s \gamma^{sca} \quad (1)$$

where n_s is the number of scatterers (entrained air voids) per unit volume, and γ^{sca} is the scattering cross section of a single scatterer, which is assumed to be a single entrained air void with spherical geometry. Note that the absorption attenuation is due to the intrinsic viscoelasticity of the cement paste matrix, and its contribution is reduced by the "missing" volume fraction which is occupied by the entrained air voids. For this simple spherical scatterer geometry, the number of scatterers, n_s is related to the volume fraction, ϕ by $\phi = \frac{4}{3}\pi a^3 n_s$, where a is the radius of the sphere. Since the entrained air voids have a (relatively) low volume fraction (under 15%), this model assumes there is no acoustic interaction between the scattered acoustic wavefields from each individual entrained air void. In addition, this model assumes that all scatterers have the same size (i.e., all have the same radius, a). Finally note that the scattering cross section, γ^{sca} is defined as the ratio of the scattered power divided by the intensity of the incident wave on a single scatter, and accounts for differences in geometry and elastic properties of the scatterer. The calculation of γ^{sca} is a classical problem and has been addressed by several researchers. This study follows Ref. [18], with calculation details given in Ref. [15].

Eq. (1) is a direct or forward model that can be used to relate the total frequency dependent attenuation, α, with the size and volume fraction of entrained air voids in a particular specimen. This model is used as part of an inversion procedure to use experimentally measured attenuation results to predict the best fit for two variables – the entrained air void size and volume (a and ϕ) for that particular specimen. Note that this inversion procedure uses the Nelder–Mead simplex method [19] on the scattering contribution (the absorption contribution is subtracted out before inversion) and is based on a model that assumes only single-sized entrained air voids (i.e., monosize per Eq. (1)). Further details on the implementation of this inversion technique are available in Ref. [15].

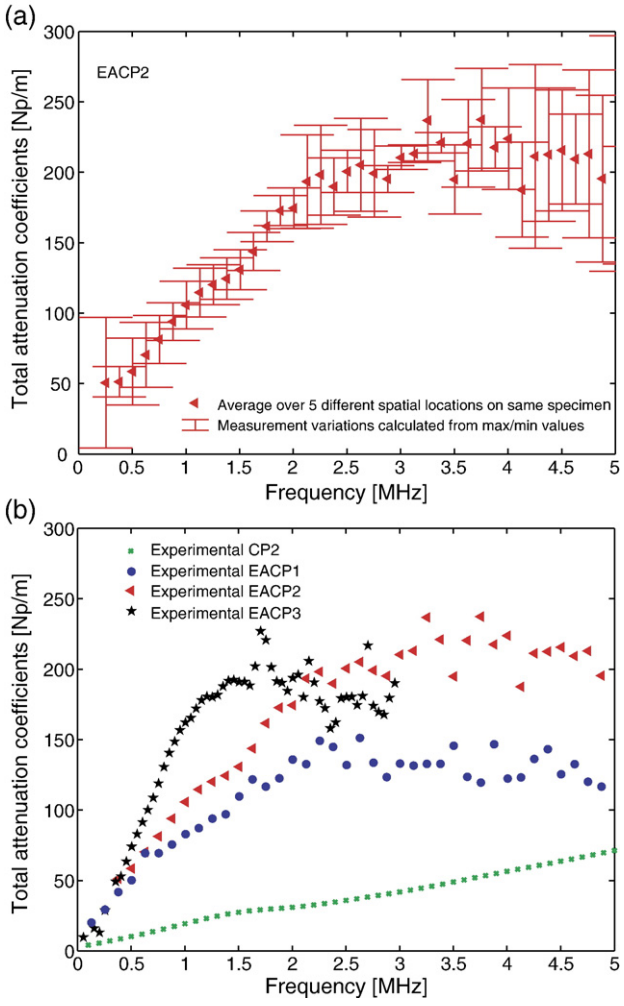

Fig. 3. The total attenuation results (a) from a typical specimen (EACP2)for a frequency bandwidth from 0.25–5 MHz (b) a summary of the (average) values for all EACP specimens plus the CP2 specimen.

3. Results and discussion

To examine the effect of air entrainment on attenuation, results from measurements on air entrained and non-air entrained cement pastes at a single w/c will be described first. Additionally, results using an inversion procedure to predict the average size and volume fraction of entrained air voids are compared to results obtained by petrography and gravimetric techniques. Then, to examine the influence of variations in the porosity inherent in cement paste on attenuation, measurements were made on neat cement pastes prepared at a range of w/c; these results are presented in Section 3.4.

3.1. Directly measured attenuation results

Attenuation measurements were made at five different spatial locations, as generally specified in Fig. 2, in each of the

seven specimen types, described in Table 1. Results obtained at these five locations were averaged to develop a frequency dependent, total attenuation curve for each specimen. Results from a typical specimen (EACP2) are shown in Fig. 3(a) for a frequency bandwidth from 0.25–5 MHz, where the error bars are based on the maximum and minimum values from all five spatial locations (at each specific frequency). Fig. 3(b) presents a summary of the average total attenuation values for all three types of EACP specimens (the three specimens prepared with the air-entraining agent), as well as the CP2 specimen, which is a cement paste specimen without air-entrainment, prepared at the same w/c as the EACP specimens. Note that error bars, which have similar trends to those presented for the EACP2 specimen in Fig. 3(a), have not been included for visual clarity.

Fig. 3(b) enables a qualitative comparison of the directly measured attenuation results in these four specimens, and clearly shows the influence of the presence of entrained air on attenuation. From this data, the attenuation is much lower in the neat cement paste specimen than all three of the entrained air specimens. It appears that the presence of entrained air voids causes significant scattering and attenuation in the frequency range examined. The attenuation in the EACP3 specimen is relatively high, which results in some scatter in the data above 1.5 MHz, as well as a limited frequency bandwidth. That is, there is no useful data above 3 MHz in this specimen.

The total attenuation in the three EACP specimens (Fig. 3(b)) appears to be directly related to the amount of air-entraining agent used (Table 1) and, hence, to the relative amount of entrained air voids contained in the paste. That is, as the air-entraining agent dosage is increased, a larger total attenuation is observed at a particular frequency. The attenuation in the neat CP2 specimen generally increases linearly with frequency, while the three EACP specimens exhibit a nonlinear behavior with frequency. These trends in behavior are predicted by fundamental scattering theory. Thus, this agreement with theory and the differences in the attenuation for the various sample types indicates that the presence and amount of entrained air voids produces measurable differences in attenuation.

3.2. Inversion results and analysis

An inversion procedure was performed on the scattering portion of the measured attenuation in the entrained air samples. Here, the absorption due to the cement paste is "removed" by subtracting the measured attenuation (α_a) in the cement paste sample produced at the same w/c (i.e., CP2). The predicted size, a and volume fraction, ϕ of entrained air voids for each specimen is presented in Table 2. The inversion predictions of volume fraction obtained by the attenuation measurements may be compared to values measured, by a trained petrographer, following ASTM C457–98, method B [5], and that from a gravimetric technique. Very good agreement between these three sets of values is noticed. The variation between the predicted entrained air void content and the petrographic results fall within the expected accuracy of ASTM C457 method B, where variations of 1 or more percent between petrographic results and measurements on fresh concrete or predicted results may be expected, according to the standard [5]. There is even better agreement between the gravimetric results (made on the fresh pastes) and the entrained air void content predicted with the ultrasound. The agreement between the predicted and measured values demonstrates the accuracy and effectiveness of using attenuation to measure entrained air void size and volume fraction in hardened cement paste.

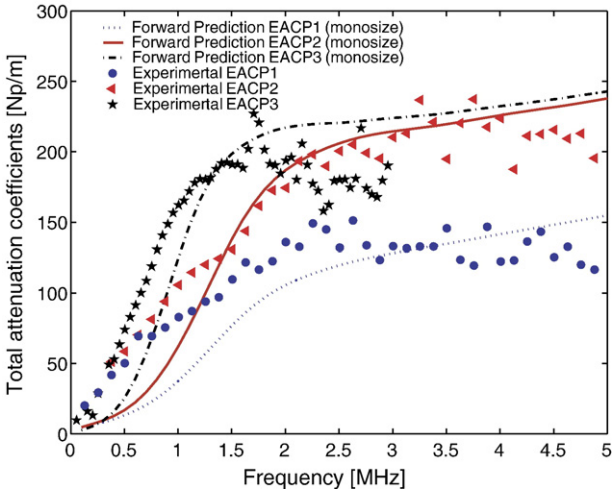

Fig. 4. Correlation plot of predicted vs. actual values of total attenuation coefficients from all EACP specimens.

However, it is worth noting that the results from the ultrasonic inversion are consistently lower than the ASTM C457–98 results, and the agreement between these two techniques improves with increasing values of ϕ. One reason for these differences could be that the petrographic results are obtained by a surface "point counting" procedure, which is likely to more accurately reflect the actual void volume when a greater number of voids are present. Thus, the petrographic results at higher void volumes may be expected to more closely match those predicted by the inversion procedure. Additionally, only a small portion of the sample (i.e., a region of a polished surface) is used to represent the entire specimen in point counting. In contrast, the ultrasonic results are "bulk," or through-thickness measurements, and use a (relatively) large volume of material to represent the entire specimen. Finally, note that ASTM C457–98 measures the total air content, sometimes with a 1 mm threshold serving as an arbitrary distinction between entrained and entrapped air, while the ultrasonic inversion procedure

Table 2
Results of ultrasonic measurement of entrained air hardened cement paste specimens in comparison with results obtained by ASTM C457–98

Name	Volume fraction, ϕ (%)			Radius, a (mm)	
	ultrasonic inversion prediction	ASTM C457–98 (method B)	Gravimetric (fresh paste)	Simplex prediction	Image analysis maximum
EACP1	3.3	4.1	3.43	0.33	0.32
EACP2	7	8.1	6.67	0.35	0.36
EACP3	11.3	12.2	11.32	0.50	0.49

isolates the contribution of the air entrained voids. As a result of these considerations, it is proposed that these ultrasonic measurements might be more representative of the actual entrained air content in the specimens.

A commercially available quantitative image analysis software package, IMAGE-PRO Plus, was used to measure the maximum size of the entrained air voids in each EACP specimen type. A "maximum" circularity index (or radius) was calculated by examining magnified digital images, similar to Fig. 1 which were obtained by optical microscopy of each sample's surface. This procedure considers five randomly selected images, each with an area of 238 mm^2, from each sample; further details on this procedure are provided in Ref. [16]. Results for the three EACP specimens are summarized in Table 2, where they are presented, for comparison, with the entrained air void sizes, a predicted with the inversion procedure. There is very good agreement between the entrained air void sizes predicted by inversion of the attenuation data, and those measured by quantitative image analysis. These results further validate the accuracy of the proposed ultrasonic procedure for characterization of cement-based materials.

3.3. Consideration of entrapped air voids

Additional insights into specimen void content and size distribution may be gained by further examination of these ultrasonic attenuation results. Consider Fig. 4, which presents a set of forward prediction results, determined by substituting the values of a and ϕ predicted by the inversion procedure with the α_a absorption attenuation measured in CP2, into the theoretical

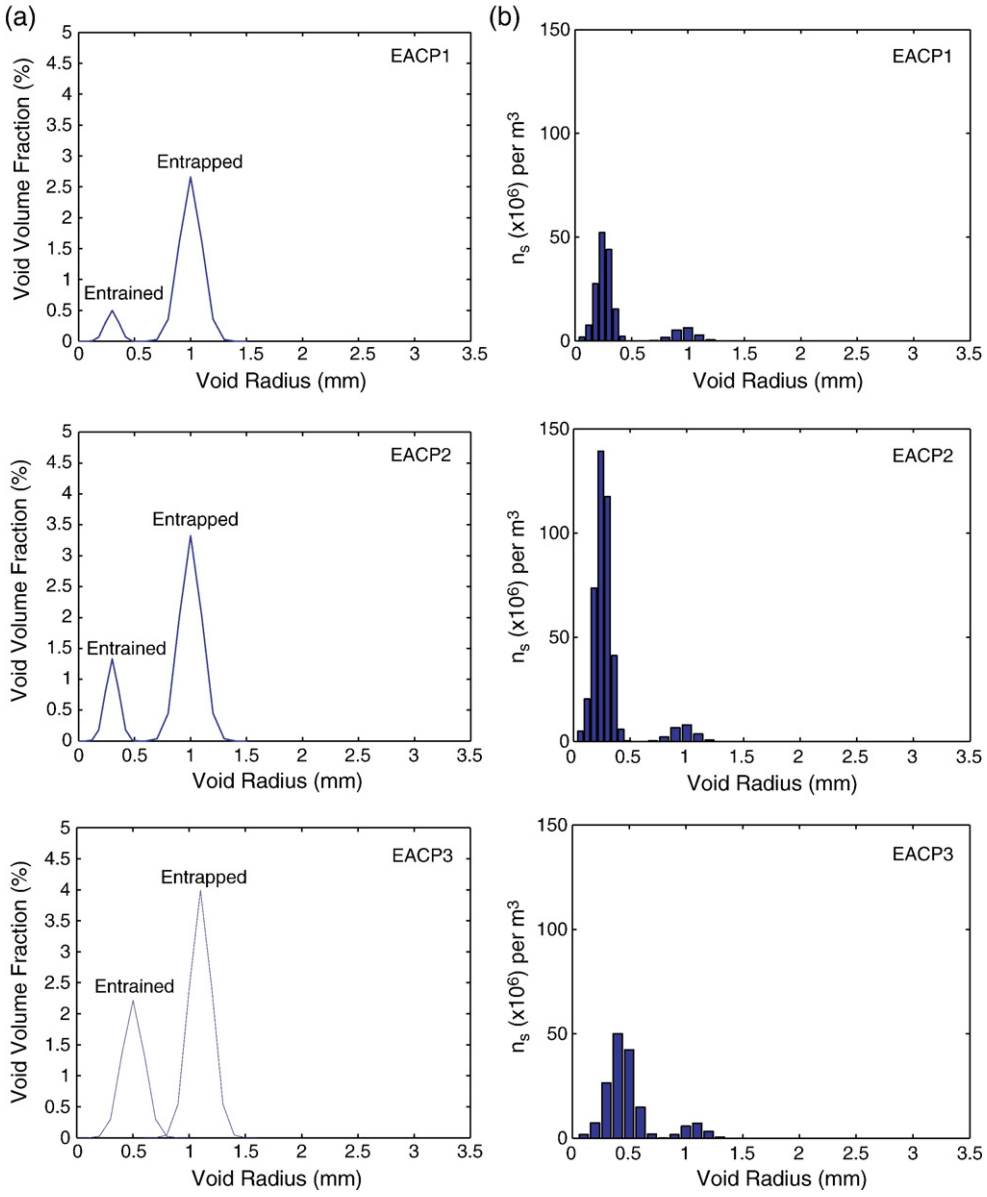

Fig. 5. Assumed two void size distribution, where the smaller radii represent the entrained air voids, and the larger radii represent the entrapped air (a) percentage of void fraction (b) number void density vs. void radius (mm).

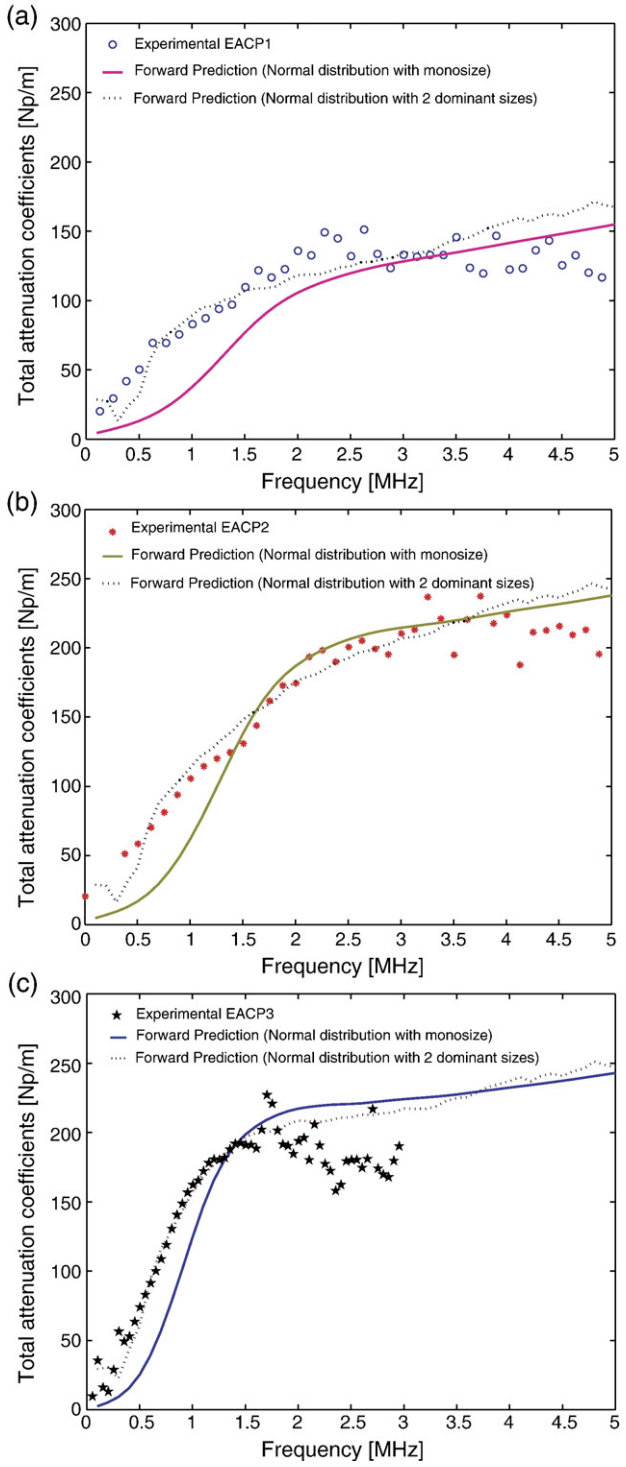

Fig. 6. Comparison of the experimentally measured attenuation with the analytical predictions using simplex optimized values ad the assumed two void size normal distributions for all the EACP1, EACP2 and EACP3 specimens.

model, Eq. (1). Comparison of these forward prediction total attenuation curves to the experimentally measured values shows general agreement between the two data sets. However, the best agreement between the predicted and measured values occurs in the frequency range 1.5–5 MHz. A possible explanation for this behavior could be the initial assumption that only a single size scatterer (i.e., entrained air voids) exists within the cement paste. It is proposed that the deviation between the predicted behavior and the measured values at low frequencies can be explained by the presence of larger, likely entrapped, air voids, which are not accounted for in the monosize scatterer model of Eq. (1).

Following Mehta and Monteiro's [20] description of the multi-scale structure of cement-based materials, a more complicated structure for the cement pastes examined may be considered. In this structure, it is assumed that two dominant void sizes exist, each having normal distributions as shown in Fig. 5. These two dominant regimes correspond to entrained and entrapped air voids, and Fig. 5(a) shows the assumed void volume fraction distribution [16]. Using this data, Fig. 5(b) shows the number of voids at a particular radius, per unit volume, which was calculated by $n_s = \frac{3\phi}{4\pi a^3}$. Note that the voids with the smaller radii represent the entrained air voids and have normal distributions centered on the radii a predicted by the inversion procedure and listed in Table 2. The second distribution of voids, with the larger radii, represent entrapped air. For simplicity, these larger entrapped air voids are assumed to be normally distributed about a single radius.

Using this two-size model for void distribution, new forward predictions may be calculated, following Ref. [21]. Results from these predictions are shown in Fig. 6(a)–(c), along with the respective experimentally measured attenuations and previously discussed monosize forward predicted values. Much better agreement is found between the experimental results and the two-size predictions, indicating that larger scatterers, likely larger entrapped air voids, are present in the EACP specimens.

3.4. Influence of w/c

Because of the importance of the attenuation due to the presence of the cement paste itself, further measurements were made on cement paste samples prepared at w/c of 0.30, 0.40, 0.50, and 0.60 to better understand the influence of intrinsic paste porosity on attenuation. Fig. 7 shows the measured total

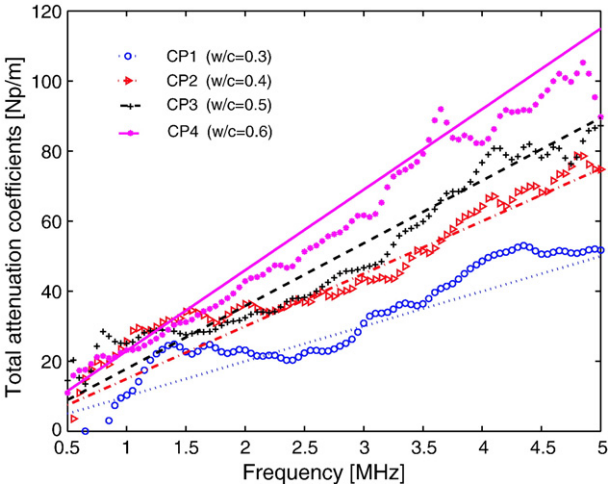

Fig. 7. Effect of w/c on frequency dependent attenuation coefficient, α (longitudinal only) measured in each type of cement paste (CP) specimen.

attenuation, α, as a function of frequency. A generally linear relationship is observed between α and frequency in Fig. 7. Also, by comparing this data for neat cement pastes with data for air-entrained pastes in Fig. 3(b), the total attenuation is much higher in the EACP samples as compared to the CP samples. Lower attenuation is expected in the cement paste (CP) samples because the scattering contribution of Eq. (1) is nonexistent in the CP specimens at these frequencies. Rather, changes in w/c are responsible for the changes in absorption attenuation, α_a in Fig. 7. This same type of linear relationship between absorption attenuation and frequency has been reported in polymers and biological tissues [23,24] and is referred to as hysteresis absorption.

It is proposed that this measured absorption attenuation behavior can be explained by considering the influence of w/c on the nano to microscale porosity of the paste. Changes in w/c are known to affect the relative volume of solids and capillary voids or pores [22]. Capillary voids, which are the irregular nano- to microscale voids which may be filled or partially filled with viscous liquid, are distinct from significantly larger entrained and entrapped air voids. The total capillary porosity in a volume of cement paste may be estimated by using the simple approach described by the Powers model. Following the approach to the Powers model presented by Mehta and Monteiro [20], the ratio of capillary voids to total solids (i.e., hydration products and unhydrated cement) for the four w/c examined is shown in Fig. 8 with a 75% degree of hydration assumed. The volume fraction of capillary voids increases and, correspondingly, the volume fraction of solids decreases – with increasing w/c.

The resulting attenuation behavior in these cement paste specimens can be qualitatively explained by considering Biot's theory [25], which describes ultrasonic wave propagation in a fluid saturated porous solid. Biot's theory may be used to consider the friction losses of a fluid as it moves within the capillary voids. Accordingly, Biot's theory qualitatively predicts an increase in absorption attenuation with an increase in the volume fraction of capillary voids in cement paste. As a result, Biot's theory can justify the experimentally observed ultrasonic behavior of increasing absorption attenuation with increasing w/c, as an increase in fluid-filled capillary voids would be expected. Further research is needed to quantify this effect and to further develop the use of absorption attenuation to quantitatively measure w/c in a range of cement-based materials.

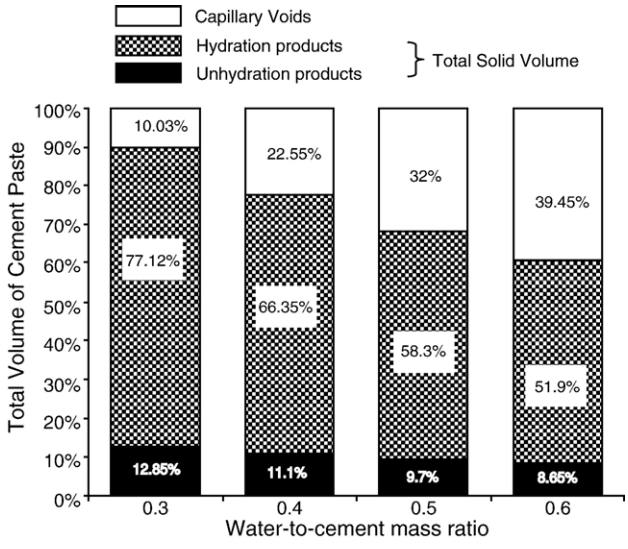

Fig. 8. Microstructural phase model of hardened cement paste comprising solids, capillary voids and air with varying water/cement ratio with 75% degree of hydration assumed.

4. Conclusions

The effectiveness of using ultrasonic attenuation as a measure of the average size and volume fraction of entrained air voids in cement paste was examined. Very good agreement was found between predictions of entrained air content, obtained from an inversion procedure based on a theoretical attenuation model, and using ultrasonic measurements, and measurements of entrained air content by standard petrographic methods and by gravimetric analysis. These results demonstrate the accuracy of using attenuation to measure the size and volume fraction of entrained air voids in hardened cement paste. These attenuation measurements were then used to suggest the existence of additional, larger entrapped air voids in the cement paste.

Because understanding the attenuation due to the inherent porosity of the cement paste is critical for developing accurate models to quantify entrained air content and size, the influence of w/c on attenuation behavior was also examined. A direct relationship between attenuation and w/c was observed. Overall, this research shows the potential of combining ultrasonic measurement techniques with theoretical wave propagation models to quantitatively characterize the multi-scale structure of cement-based materials.

Note that this study considers only a real, but simplified, cement-based material – cement paste. An understanding of attenuation in this material is a critical step towards the quantitative modeling of ultrasonic wave propagation in concrete components. By taking a fundamental, mechanics-based approach, it should be possible to add additional components (such as scattering by fine and coarse aggregate [26]) in a systematic fashion and eventually build a realistic (predictive) model for ultrasonic wave propagation in concrete. Finally, it should be possible to extend this technique to characterize multi-scale porosity in the fresh state.

Acknowledgements

This research is partially supported by the Georgia Department of Transportation and the conclusions expressed herein are those of the authors and do not necessarily represent the opinions or conclusions of the Georgia Department of Transportation. A Royal Thai Government Scholarship was provided to W. Punurai. The authors would like to thank Mr. Terry Vines, a trained and certified petrographer at Lafarge in Atlanta, GA for performing the petrographic analysis. **[KS]**

References

[1] ACI 318. Manual of Concrete Practice Part 3: Building Code Requirements for Structural Concrete and Commentary, ACI, Farmington Hills, MI, 2005.

[2] ASTM C138. Standard Test Method for Unit Weight, Yield, and Air Content (Gravimetric) of Concrete, American Society of Testing and Materials, Philadelphia, PA, 1992.

[3] ASTM C173. Air Content of Freshly Mixed Concrete by the Volumetric Method, American Society of Testing and Materials, Philadelphia, PA, 1994.

[4] ASTM C231. Standard Test Method for Air Content of Freshly Mixed Concrete by the Pressure Method, American Society of Testing and Materials, Philadelphia, PA, 1991.

[5] ASTM C457-98. Standard Test Method for Microscopical Determination of Parameters of the Air-void System in Hardened Concrete, Amer Soc Test Mater, West Conshohocken, PA, 2000.

[6] S. Zhihui, Y. Guang, S.P. Shah, Microstructure and early-age properties of Portland cement paste – effects of connectivity of solid phases, ACI Mater. J. 102 (2005) 122–129.

[7] S. Popovics, J.S. Popovics, Ultrasonic testing to determine water to cement ratio for freshly mixed concrete, Cem. Concr. Aggr. 20 (1998) 262–268.

[8] M.G. Hernandez, J.J. Anaya, L.G. Ullate, M. Cegarra, T. Sanchez, Application of a micromechanical model of three phases to estimating the porosity of mortar by ultrasound, Cem. Concr. Res. 36 (2006) 617–624.

[9] L. Vergara, R. Miralles, J. Gosalbez, F.J. Juanes, L.G. Ullate, J.J. Anaya, M.G. Hernandez, M.A.G. Izquierdo, NDE ultrasonic methods to characterise the porosity of mortar, NDE & E Int. 34 (2001) 557–562.

[10] M. Goueygou, S. Piwakowski, S. Ould Naffa, F. Buyle-Bodin, Assessment of broadband ultrasonic attenuation measurements in inhomogeneous media, Ultrasonics 40 (2002) 77–82.

[11] D.G. Aggelis, T.P. Philippidis, Ultrasonic wave dispersion and attenuation in fresh mortar, NDT & E Int. 37 (2004) 617–631.

[12] H.W. Reinhardt, C.U. Grosse, Continuous monitoring of setting and hardening of mortar and concrete, Constr. Build. Mater. 18 (2004) 145–154.

[13] Z. Lafhaj, M. Goueygou, A. Djerbi, M. Kaczmarek, Correlation between porosity, permeability and ultrasonic parameters of mortar with variable water/cement ratio and water content, Cem. Concr. Res. 36 (2006) 625–633.

[14] M. Shickert, Ultrasonics NDE of concrete, IEEE Ultras Symp. Proc., vol. 1, 2002, pp. 739–748.

[15] W. Punurai, J. Jarzynski, J. Qu, K.E. Kurtis, L.J. Jacobs, Characterization of entrained air voids with scattered ultrasound, NDT & E Int. 39 (2006) 514–524.

[16] Punurai W. Cement-based materials' characterization using ultrasonic attenuation. Ph.D. Dissertation, Georgia Institute of Technology, Atlanta, May 2006.

[17] S. Biwa, Independent scattering and wave attenuation in viscoelastic composites, Mech. Mater. NDT & E Int. 33 (2001) 635–647.

[18] C.F. Ying, R. Truell, Scattering of a plane longitudinal wave by a spherical obstacle in an isotropically elastic solid, J. Appl. Phys. 27 (1956) 1086–1097.

[19] J.A. Nelder, R. Mead, A simplex method for function minimization, Comput. J. 7 (1956) 308–313.

[20] P.K. Mehta, P.J.M. Monteiro, Concrete: Microstructure, Properties, and Materials, first editionMcGraw Hill, New York, 1993.

[21] C.M. Sayers, R.L. Smith, The propagation of ultrasound in porous media, J. Ultrason. 20 (1982) 201–205.

[22] D.M. Roy, P.W. Brown, D. Shi, B.E. Scheetz, W. May, Concrete microstructure porosity and permeability, Strat Hwy Res Prog. Report SHRP-C-628, Nat Res Counc, Washington, DC, 1993.

[23] Y.C. Fung, A First Course in Continuum Mechanics, third ed., Prentice Hall, New Jersey, 1993.

[24] B. Hartmann, J. Jarzynski, Ultrasonic hysteresis absorption in polymers, J. Appl. Phys. 43 (1972) 4304–4312.

[25] M.A. Biot, Mechanics of deformation and acoustic propagation in porous media, J. Appl. Phys. 33 (1962) 1482–1498.

[26] L.J. Jacobs, J. Owino, Effect of aggregate size on attenuation of Rayleigh surface waves in cement-based materials, J. Eng. Mech. 97 (2000) 58–65.